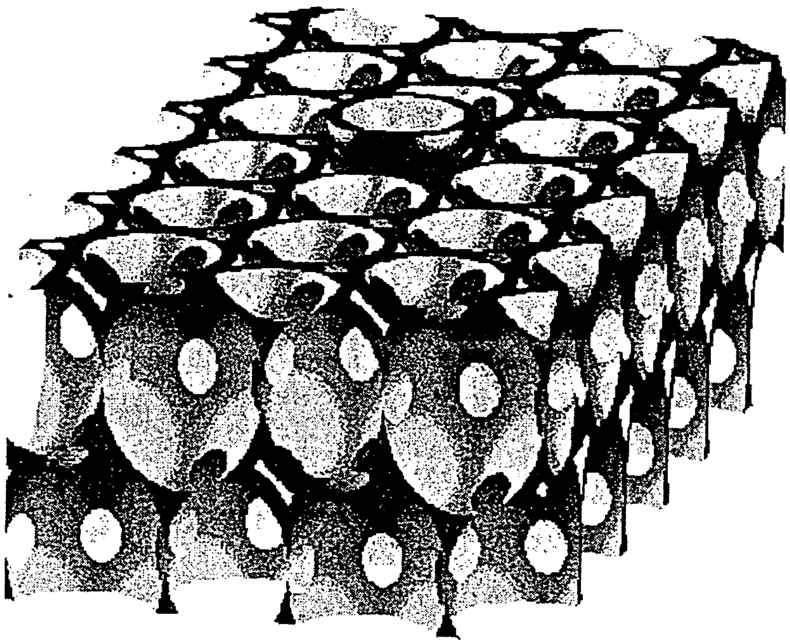

Figure 1:
Cross-sectional view through the inverse opal backbone (blue) resulting from incomplete infiltration of silicon into the air voids of an artificial opal. After etching out the template, a fcc lattice of overlapping air spheres remain and additional air voids appear as triangular or diamond shaped holes on the surface of the cut. A tunable PBG is obtained by infiltrating this backbone with nematic liquid crystal (yellow) which wets the inner surface of <u>each</u> sphere (only one is shown in the figure).

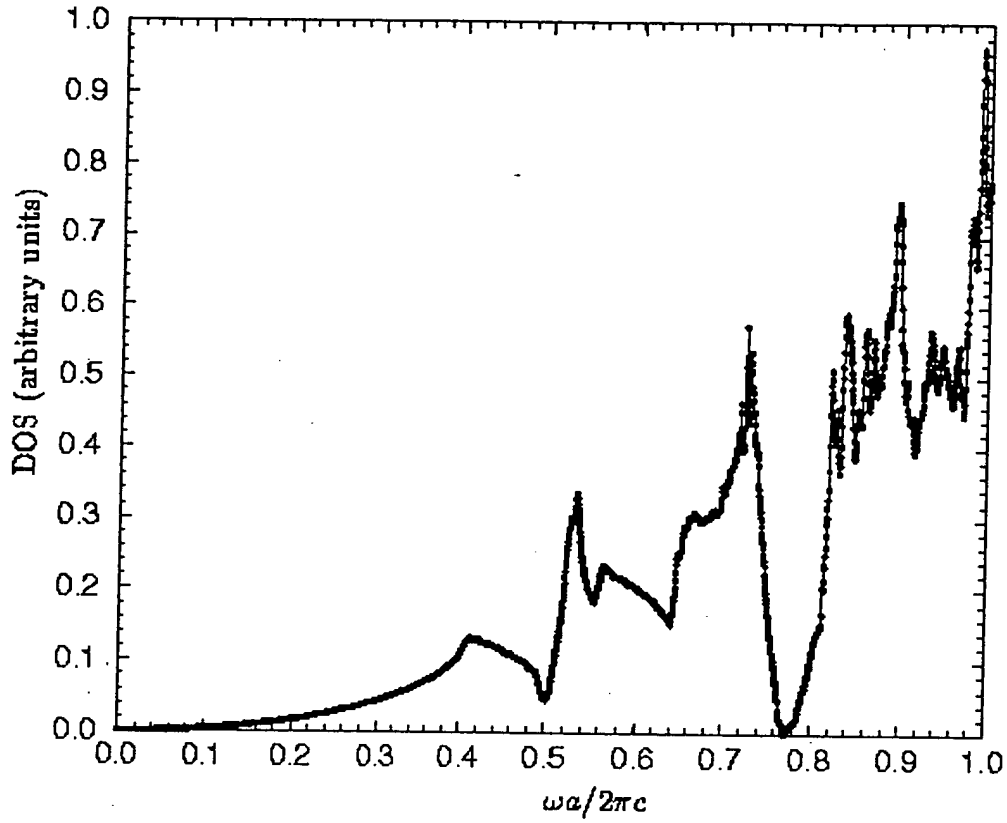

Figure 2: Total DOS for an inverse opal which is infiltrated with a nematic liquid crystal. The nematic director is orientated along the (0,0,1) axis of the inverse opal backbone. The inverse opal backbone is made of silicon (24.5% by volume) which is in filtrated with the liquid crystal BEHA (36.8% by volume). The isotropic refractive index of silicon is $n_{Si}=3.4$ and the principal refractive indices of BEHA are $n_{LC}^{\parallel}=1.6$ and $n_{LC}^{\perp}=1.4$.

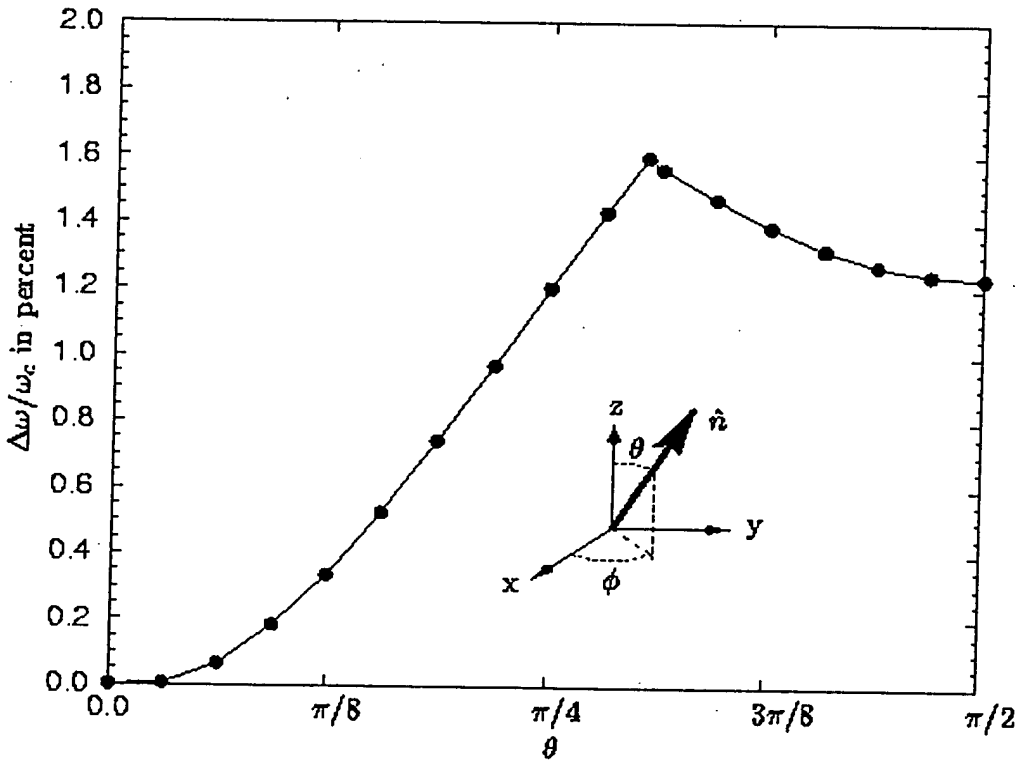

Figure 3: Dependence of the photonic band gap size for a silicon inverted opal infiltrated with the nematic liquid crystal (BEHA) on the orientation of the nematic director $\hat{n}(\phi,\vartheta)$ for fixed angle $\phi=\pi/4$. The volume fractions are the same as in Fig. 2.

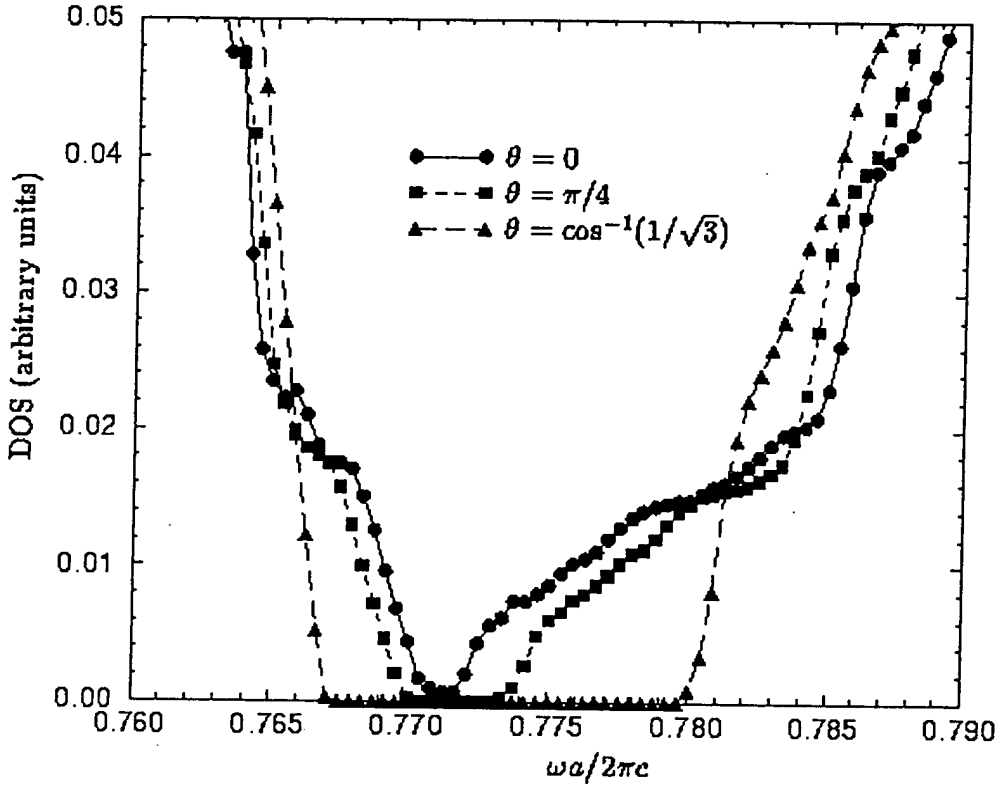

Figure 4: Total photon DOS for a silicon inverse opal which is infiltrated with the nematic liquid crystal (BEHA) for various orientations of the nematic director $\hat{n}(\phi,\vartheta)$. The angle $\phi=\pi/4$ is fixed and the volume fractions are the same as in Fig. 2. The PBG is closed for $\vartheta=0$ but reaches a maximum value $\Delta\omega/\omega_c \approx 1.6\%$ relative to its center frequency ω_c for $\hat{n}=(1,1,1)/\sqrt{3}$.

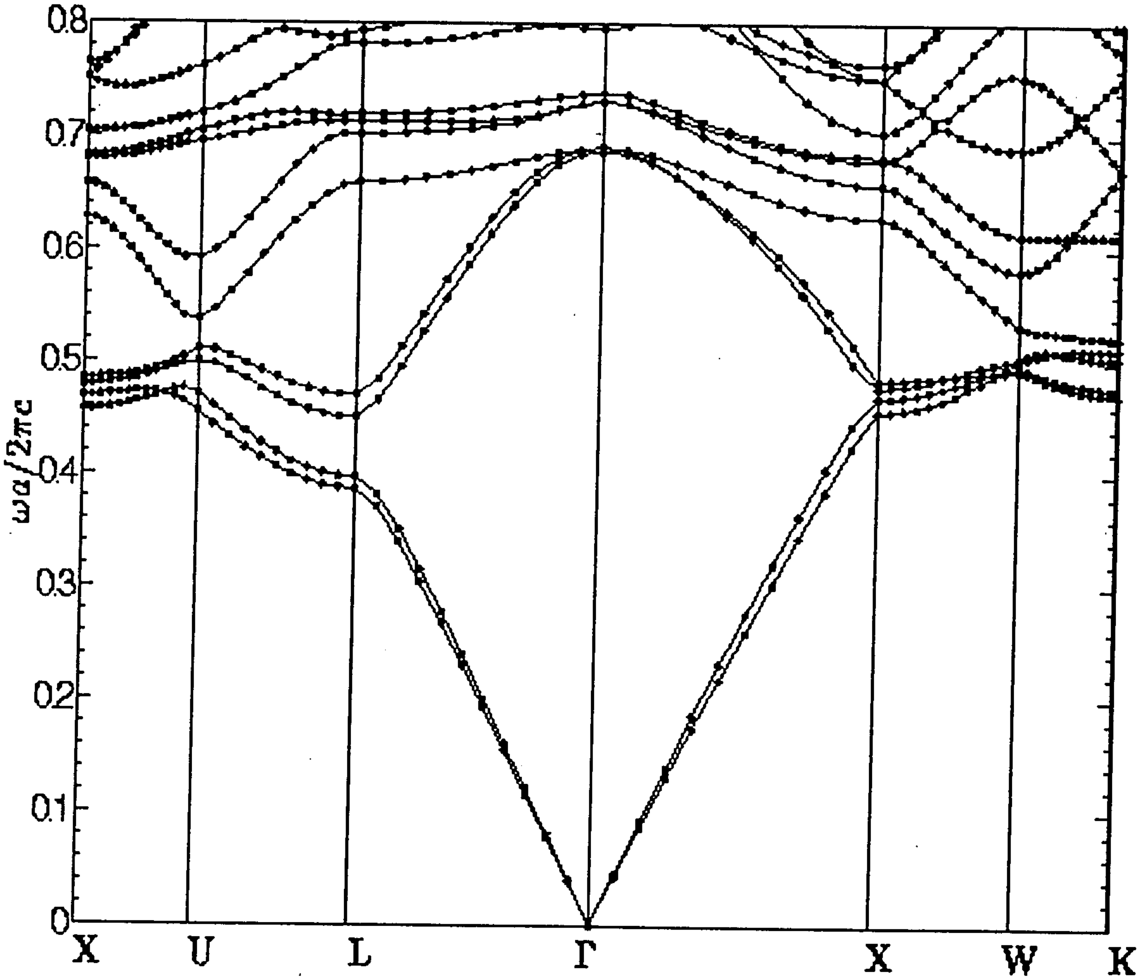

Figure 5. Photonic band structure of a silicon inverse opal which has been fully infiltrated with liquid crystal BEHA

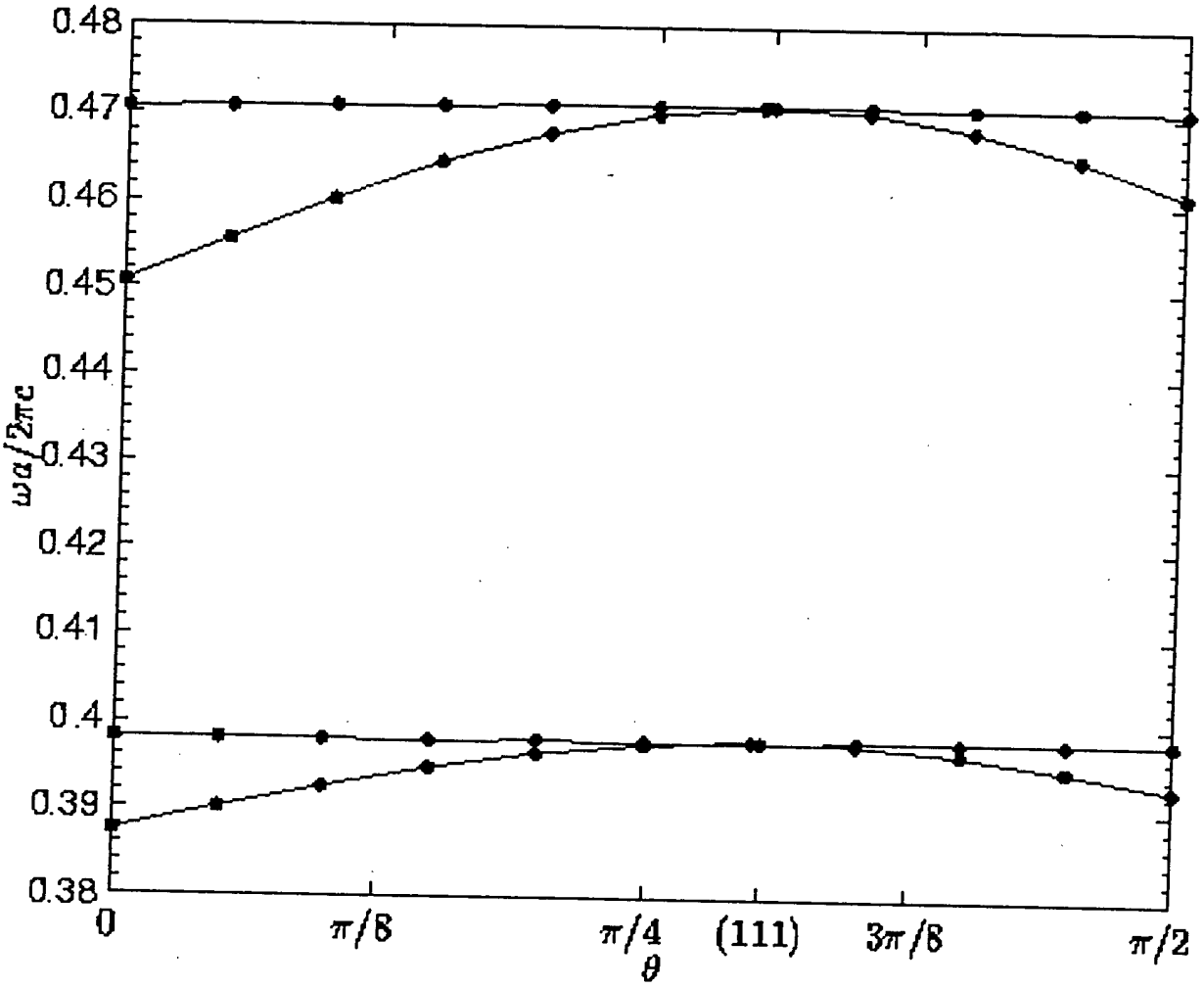

Fig 6. Variation at the L-point: Bands 1-4

Figure 7: Variation at the L-point: Bands 6-10

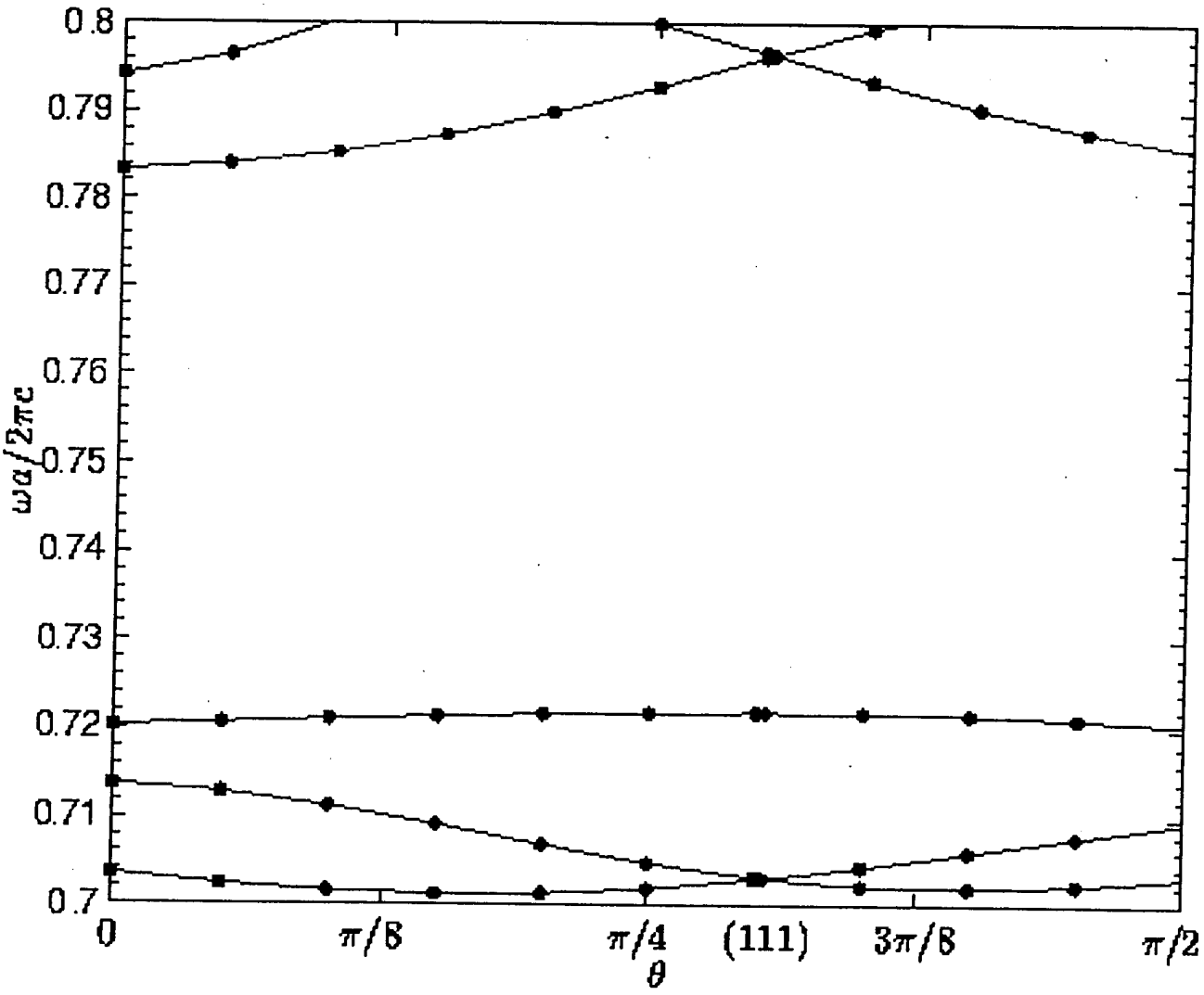

Figure 8: Variation at the X point: Bands 1-4

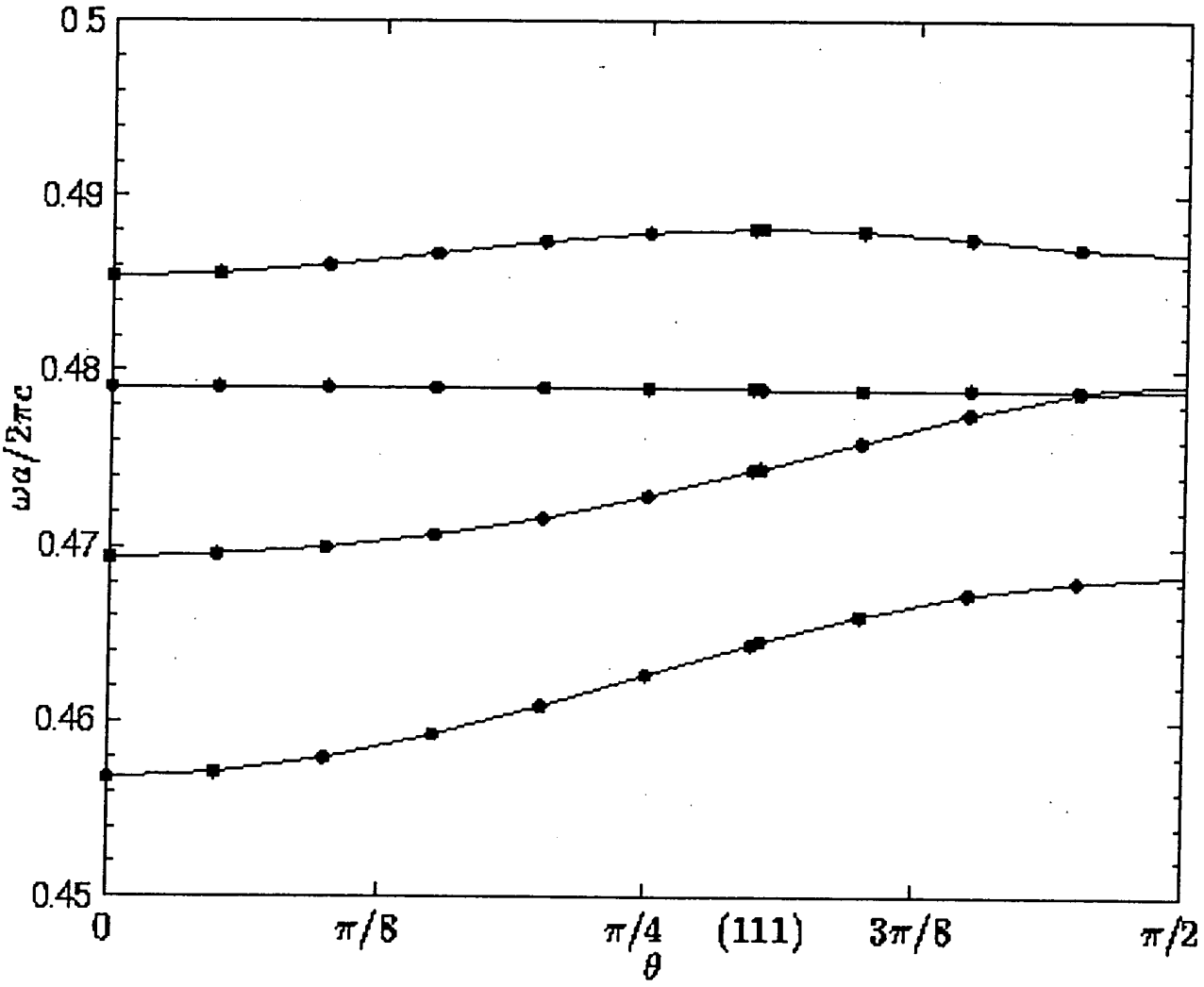

Fig 9. Variation at the W-point: Bands 1-4

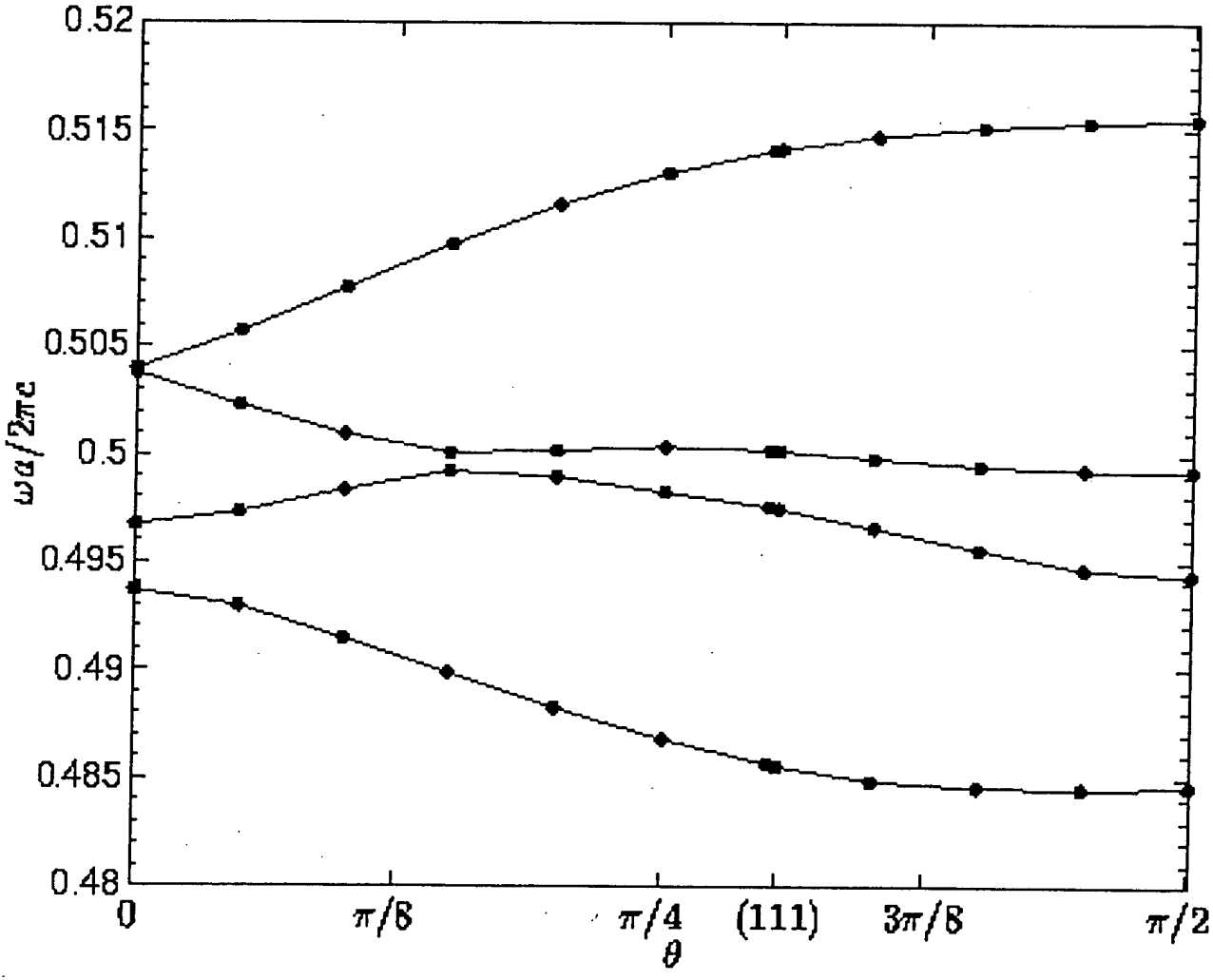

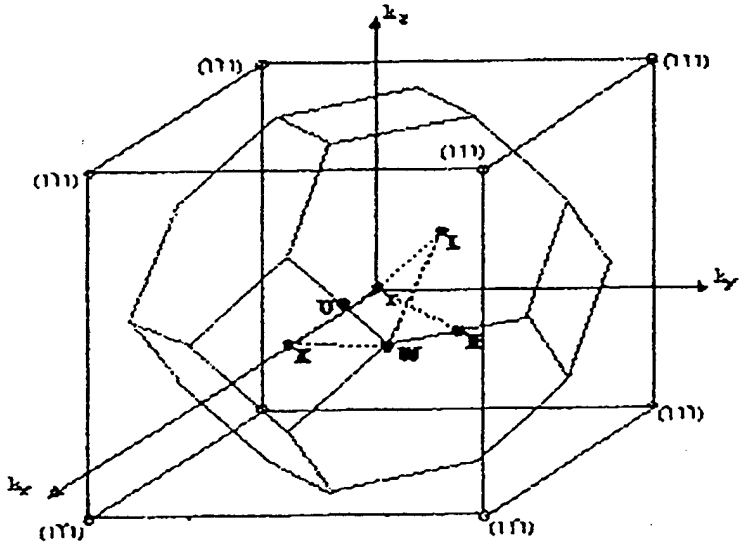

FIG. 10

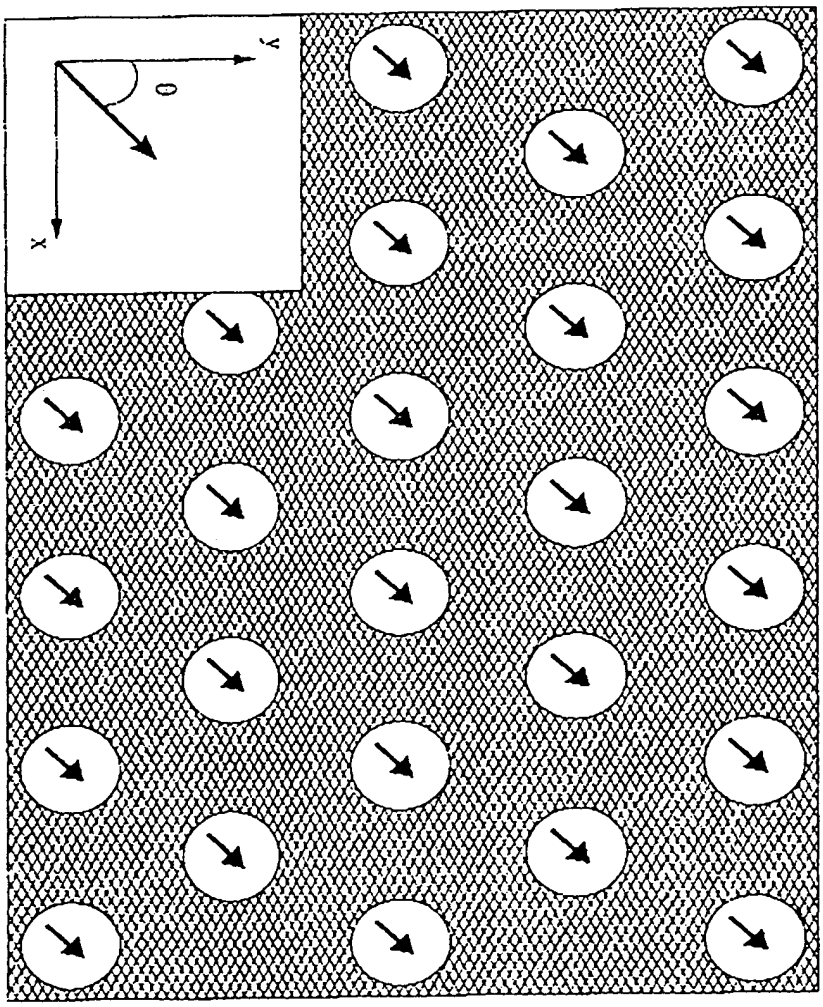

FIG. 11

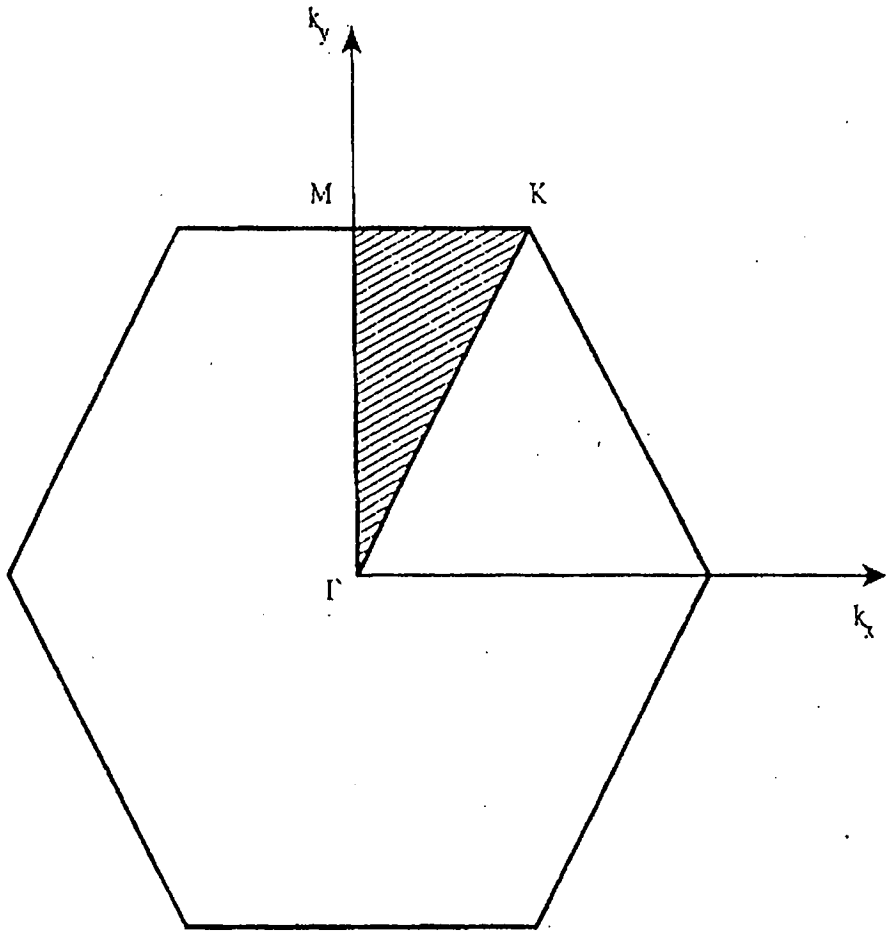

FIG. 12

FIG. 13

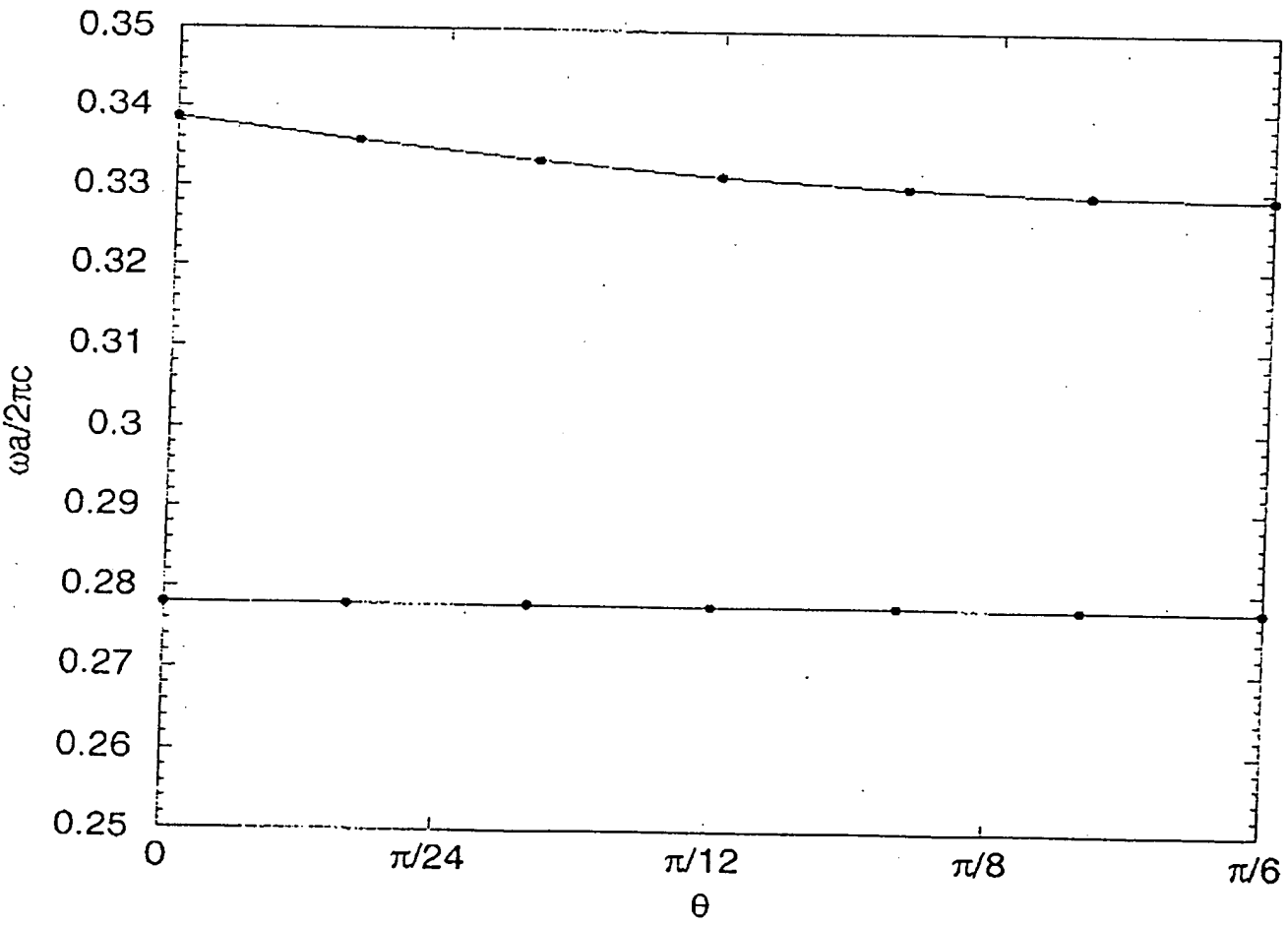

FIG. 14

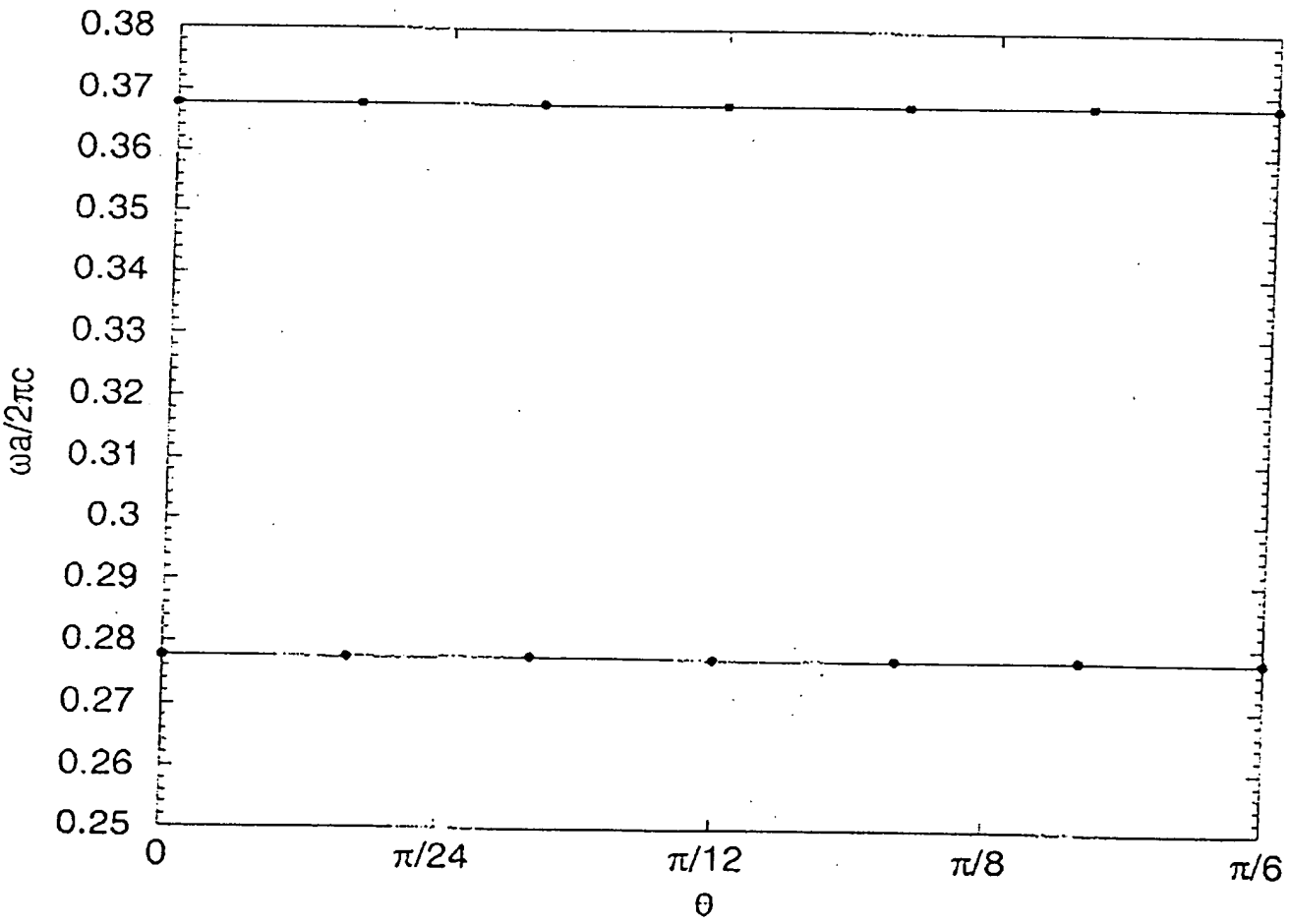
0.38
0.37
0.36
0.35
0.34
0.33
0.32
0.31
0.3
0.29
0.28
0.27
0.26
0.25
ωa/2πc
0
π/24
π/12
π/8
π/6
θ

FIG. 15

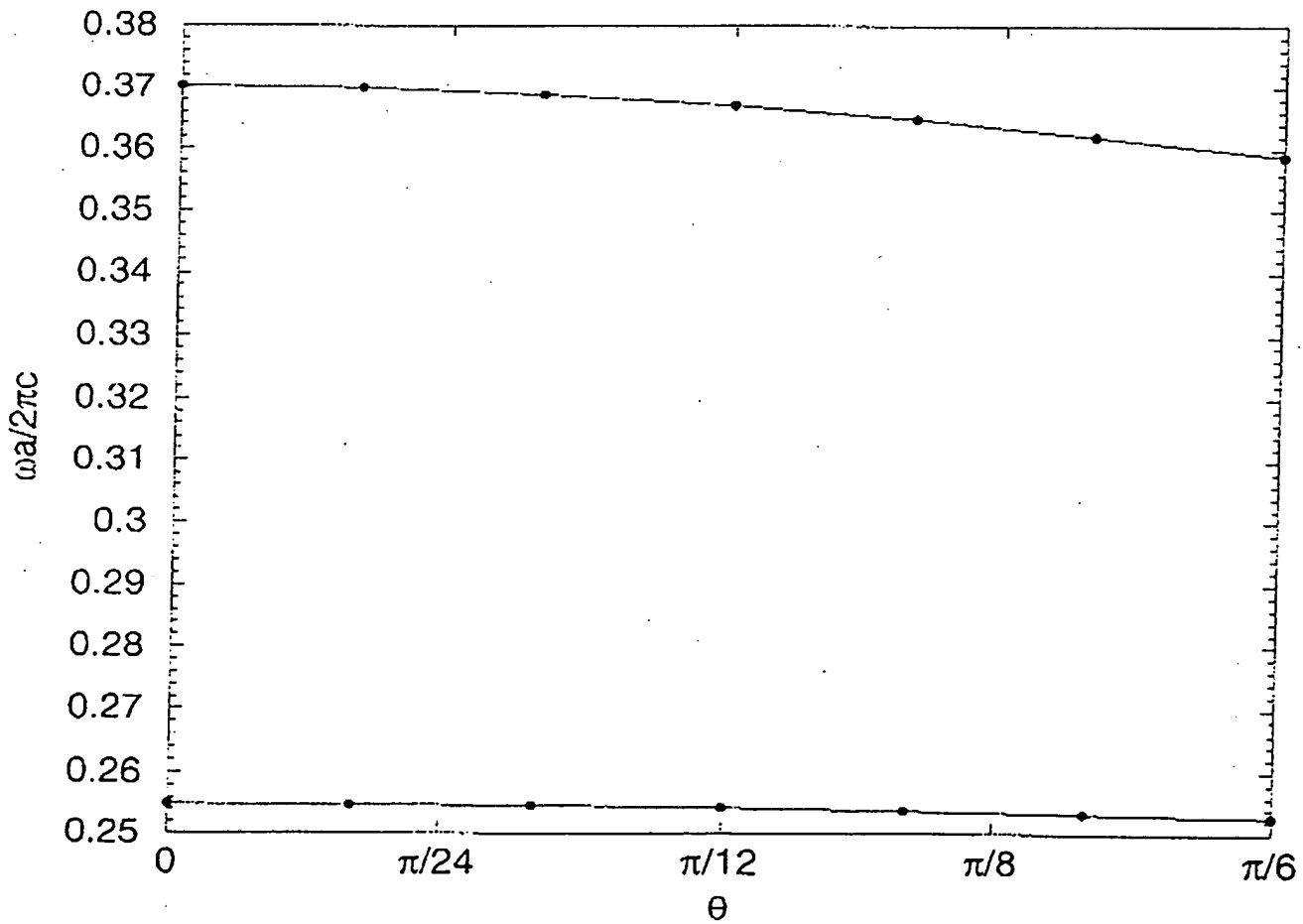
0.38
0.37
0.36
0.35
0.34
0.33
0.32
0.31
0.3
0.29
0.28
0.27
0.26
0.25
ωa/2πc
0
π/24
π/12
π/8
π/6
θ

FIG. 16

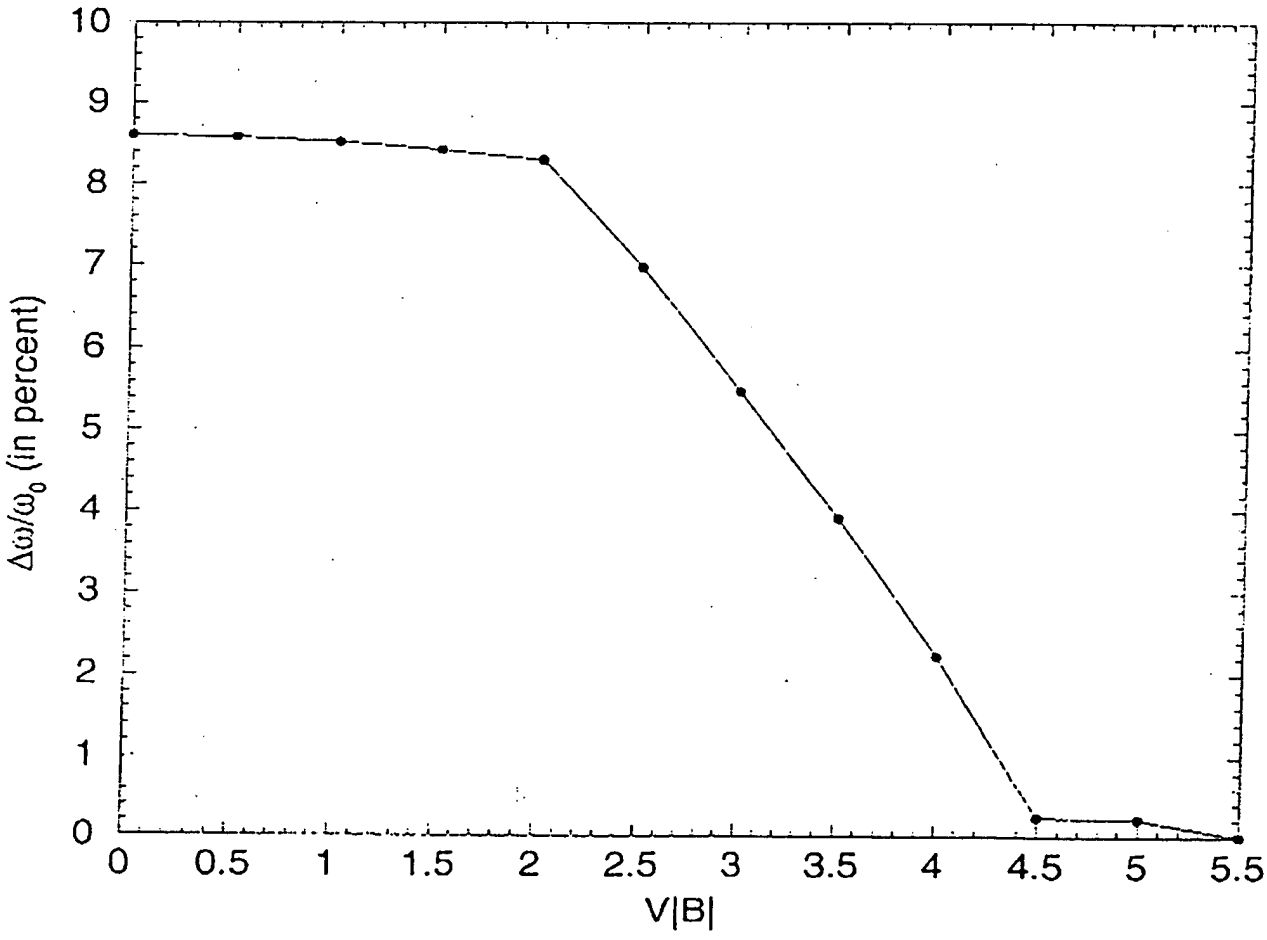

FIG. 17